Extension of equilibrium turbulent heat flux models to high-speed shear flows

RODNEY D. W. BOWERSOX†

Department of Aerospace Engineering, Texas A&M University, College Station, TX 77843, USA

An algebraic heat flux truncation model was derived for high-speed gaseous shear flows. The model was developed for high-temperature gases with caloric imperfections. Fluctuating dilatation moments were modelled via conservation of mass truncations. The present model provided significant improvements, up to 20 %, in the temperature predictions over the gradient diffusion model for a Mach number ranging from 0.02 to 11.8. Analyses also showed that the near-wall dependence of the algebraic model agreed with expected scaling, where the constant Prandtl number model did not. This led to a simple modification of the turbulent Prandtl number model. Compressibility led to an explicit pressure gradient dependency with the present model. Analyses of a governing parameter indicated that these terms are negligibly small for low speeds. However, they may be important for high-speed flow.

1. Introduction

Algebraic truncation models provide a possibility for bridging resolved and unresolved turbulence in the simulation of high-Reynolds-number turbulence. The objective of this study was to further develop algebraic heat flux truncation models for high-speed shear flows. Convective heat transfer has been the subject of considerable investigation; as such reviews are available elsewhere, e.g. Kays & Crawford (1993). A brief synopsis of the models of relevance to the present study is given here. The turbulent heat flux q_i^T is often approximated with a gradient diffusion model $q_i^T = -\mu_T \tilde{h}_{,i}/Pr_T$, where μ_T is the turbulent viscosity, $\tilde{h}$ is the mass-weighed mean enthalpy and Pr_T is the turbulent Prandtl number. A limitation of this approach is the inability to predict realistic values for all three components of the heat flux as it aligns the scalar flux with the mean scalar gradient. Algebraic models based on truncating the transport equation for the turbulent heat flux have been developed to overcome this limitation (Wikstrom, Wallin & Johansson 2000). Launder (1988) proposed a model by assuming that the heat flux was proportional to the production times a time scale. The resulting constant density, constant specific heat, model is given by $q_i^T = C_T \tau_u (\tau_{ik}^T C_p \bar{T}_{,k} - q_k^T \bar{u}_{i,k})$. In this expression, C_T is a constant (≈ 0.3), τ_u is a relaxation time scale, τ_{ij}^T is the Reynolds shear stress, C_p is the specific heat at constant pressure, $\bar{T}$ is the mean temperature, and $\bar{u}$ is the mean velocity. Inclusion of the second term on the right-hand side leads to essentially correct predictions of the axial and transverse heat flux for pipe, jet and homogeneous shear flows (Launder 1988). The above models are often extended to high-speed flow, via Morkovin's (1961)

† Email address for correspondence: bowersox@aeromail.tamu.edu

hypothesis. For the algebraic models, this extension implicitly assumes that both the mean Favre enthalpy fluctuation $\overline{h''}$ and the fluctuating dilatation $u''_{k,k}$ are negligible.

2. Governing equations

Most high-speed simulations are based on the Favre (1969) averaged conservation equations. The two moments that require models are the turbulent shear stress $\tau^T_{ij} = -\overline{\rho u''_i u''_j}$ and heat flux $q^T_i = \overline{\rho h'' u''_i}$; this is, the case when the turbulent kinetic energy $k^T = \frac{1}{2}\overline{u''_i u''_i}$ equation is combined with the averaged static energy equation to eliminate the dissipation and pressure fluctuation terms, and the diffusion and convection of k^T are considered negligible in the resulting mean equation.

The present modelling was performed on the energy flux $\vartheta^T_i = \overline{\rho e'' u''_i}$ transport equation. This choice, over enthalpy, was based on the elimination of ambiguous moments with the unsteady pressure. Taking moments between the energy and momentum equations resulted in the following transport equation:

$$\frac{D\vartheta^T_i}{Dt} = \tau^T_{ik}\tilde{e}_{,k} - \vartheta^T_k \tilde{u}_{i,k} - \overline{p(u''_i u''_{k,k})} - [(\overline{p'u''_i}) + \overline{u''_i}\,\bar{p}]\tilde{u}_{k,k} + \overline{p'e''_{,i}} - \overline{e''}\,\bar{p}_{,i} + \bar{\rho}\xi_i. \quad (2.1)$$

In this expression, the left-hand side is $D\vartheta^T_i/Dt \equiv \vartheta^T_{i,t} + (\vartheta^T_i \tilde{u}_k)_{,k}$, the overbar denotes a time-averaged quantity, the overtilde denotes a Favre averaged quantity, the superscript T denotes a turbulence moment, the double and single primes denotes a fluctuating quantity under Favre averaging and time averaging, respectively. The variables are defined as follows: ρ is the density, u_i is the velocity vector, p is the pressure, $\bar{\tau}_{ik}$ is the molecular shear stress tensor, e is the internal energy, h is the enthalpy and $\bar{q}_i$ is the molecular heat flux vector. The triple correlations, molecular, diffusion and dissipation terms are all grouped into $\bar{\rho}\xi_i$. The physical interpretation of the terms in (2.1) follows from Launder (1988). The exceptions are the compressibility terms, specifically, the third, fifth and seventh terms on the right-hand side. Simplifications to eliminate the pressure fluctuations were performed using state equations.

For thermally perfect gases with caloric imperfections, the caloric equations of state are functions of translational temperature. For many cases, $C'_v/\bar{C}_v \ll e''/\tilde{e}$. Hence, $e'' \simeq \bar{C}_v T''$, where $\bar{C}_v$ is the value of the specific heat at the mean temperature $\tilde{T}$. Thus, the mean and fluctuating thermal equations of state reduce to

$$\bar{p} = (R/\bar{C}_v)\bar{\rho}\tilde{e}, \quad p' = (R/\bar{C}_v)(\tilde{e}\rho' + \rho e''). \quad (2.2)$$

3. Modelling simplifications

3.1. Simplifications to the energy flux transport equation

Equation (2.1) was simplified as follows. First, a model was derived for the velocity dilatation by taking a moment of the fluctuating conservation of mass equation. Neglecting unsteady and third-order terms, and simplifying with the identity $\overline{\rho_{,k}u''_i} + \overline{\rho u''_{i,k}} = 0$, resulted in $\overline{\rho u''_i u''_{k,k}} \simeq -\overline{\rho u''_i u''_k}\bar{\rho}_{,k}/\bar{\rho} + \tilde{u}_k\overline{\rho u''_{,k}}$, where $\tilde{u}_k\overline{\rho u''_{,k}}$ is expected to be small for shear layers. Neglecting this term ensured Galilean invariance. The resulting model is

$$\bar{\rho}\overline{u''_i u''_{k,k}} \simeq \tau^T_{ik}\bar{\rho}_{,k}/\bar{\rho}. \quad (3.1)$$

This relation is equivalent to the leading term in the Ristorcelli (1993) model. Comparison of (3.1) to the Mach 2.25 adiabatic wall direct numerical simulation
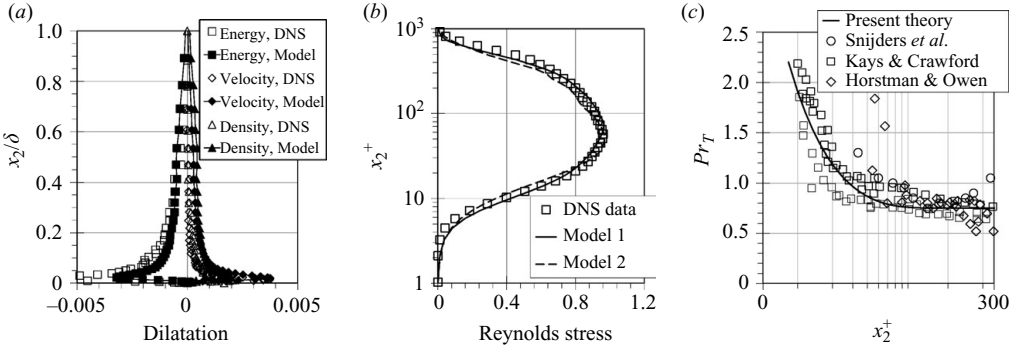
FIGURE 1. Supporting evidence for model simplifications. (*a*) Comparison of the present velocity, energy and density dilatation models (3.1) and (3.9) to the DNS data of Pirozzoli, Grasso & Gatski (2004), $M = 2.25$, Air, $T_w/T_{aw} = 1.0$, $Re = 4000$; (*b*) Comparison of the Reynolds stress correlations – model 1: (3.13), model 2: (3.14), normalized by the wall shear stress, to DNS data; (*c*) Comparison of the modified turbulent Prandltl number (defined in (3.15)) to the experimental data of Snijders, Koppius & Nieuwvelt (1983), Kays & Crawford (1993), includes flat plate and pressure gradient data, and Horstman & Owen (1972).

(DNS) data, shown in figure 1(*a*), indicated the approximations were reasonable. Second, the terms in the square brackets in (2.1) were reduced with the state equation to

$$\overline{p'u_i''} = -\bar{p}\overline{u_i''} + (R/\bar{C}_v)\vartheta_i^T. \tag{3.2}$$

Third, $\overline{p'e_{,i}''}$ was estimated to be of second-order diffusion by using (2.2) to write $\overline{p'e_{,i}''} = R\left[\bar{\rho}\overline{e''e_{,i}''} + \tilde{e}\overline{\rho'e_{,i}''} + \right]/\bar{C}_v$. The first term is a gradient of the energy variance. The second term was also shown to be proportional to gradients of statistical moments by approximating the internal energy and density fluctuations with a Taylor series, noting that $\overline{\rho'e''} = \overline{\rho'e'} = -\bar{\rho}\overline{e''}$ and assuming that statistical moments were approximately homogeneous. With this simplification, the incompressible pressure scrambling effect (e.g. Launder 1976; Pope 1983) is omitted; the implication of this is discussed in § 3.4. With these simplifications, (2.1) was written as

$$D\vartheta_i^T/Dt = \tau_{ik}^T(\tilde{e}_{,k} - \bar{p}\bar{\rho}_{,k}/\bar{\rho}) - \vartheta_k^T\tilde{u}_{i,k} - (R/\bar{C}_v)\vartheta_i^T\tilde{u}_{k,k} - \overline{e''}\bar{p}_{,i} + \bar{\rho}\xi_i. \tag{3.3}$$

3.2. *Algebraic energy flux model*

An algebraic model for the energy flux was obtained by truncating (3.3) following Girimaji & Balachander (1998). Defining an energy flux correlation coefficient $F_i = \vartheta_i^T/[(\bar{\rho}k^T)^{1/2}(\bar{\rho}\overline{e''^2})^{1/2}]$, neglecting $\bar{\rho}\xi_i$, and performing the operations led to

$$\vartheta_i^T/\tau_\vartheta \approx \tau_{ik}^T\tilde{\psi}_{,k} - \vartheta_k^T\tilde{u}_{i,k} - (R/\bar{C}_v)\vartheta_i^T\tilde{u}_{k,k} - \overline{e''}\bar{p}_{,i}, \tag{3.4}$$

where

$$\tilde{\psi}_{,k} = \tilde{e}_{,k} - \bar{p}\bar{\rho}_{,k}/\bar{\rho}^2 = \tilde{h}_{,k} - \bar{p}_{,k}/\bar{\rho}. \tag{3.5}$$

In (3.4), $\tau_\vartheta^{-1} = \frac{1}{2}[(P^{k^T} - \bar{\rho}\varepsilon)/\bar{\rho}k^T + (P^{\overline{e''2}} + \bar{\rho}\chi)/\frac{1}{2}\bar{\rho}\overline{e''^2}]$, where $P^{()}$ denotes the production and χ is the dissipation rate for the energy fluctuation variance $\overline{e''^2}$. To build an algebraic model, the system was further simplified by assuming that $\tau_\vartheta \approx \sigma_\vartheta k^T/\varepsilon$, where σ_ϑ was added as an adjustable constant. Thus, (3.4) was reduced to

$$a_{ik}\vartheta_k^T = b_i, \tag{3.6}$$

where

$$a_{ik} = \left[\tau_\vartheta^{-1} + (R/\bar{C}_v)\tilde{u}_{m,m}\right]\delta_{ik} + \tilde{u}_{i,k}, \quad b_i = \tau_{ik}^T \tilde{\psi}_{,k} - \overline{e''}\,\bar{p}_{,i}. \tag{3.7}$$

Equation (3.6) was explicitly solved for ϑ_i^T. The determinant was approximated as τ_ϑ^{-3} for shear flows with a principal strain rate, which also helped with numerical stability.

To account for the second term on the right-hand side of b_i in (3.7), the following transport equation was derived for $\overline{e''}$ from the conservation of energy

$$D\bar{\rho}\overline{e''}/Dt = -\bar{\rho}\tilde{e}_{,k}\overline{u_k''} + \vartheta_{k,k}^T - \bar{\rho}\overline{u_k''e_{,k}''} - \tau_{kl}^T\tilde{u}_{l,k} - (\bar{p}\overline{\rho'u_{k,k}''} + \tilde{u}_{k,k}\overline{\rho'p'})/\bar{\rho} + M. \tag{3.8}$$

On the left-hand side of this expression, $D\bar{\rho}\overline{e''}/Dt \equiv (\bar{\rho}\overline{e''})_{,t} + (\bar{\rho}\tilde{u}_k\overline{e''})_{,k}$. The production and redistribution terms were listed on the right-hand side, and the molecular fluctuation terms were grouped in M. The second and third terms on the right-hand side were expressed as $\vartheta_{k,k}^T - \bar{\rho}\overline{u_k''e_{,k}''} = \vartheta_k^T\bar{\rho}_{,k}/\bar{\rho} + \overline{\rho e''u_{k,k}''}$ to second order, with the product rule. To close the equation, energy and density dilation models were derived following the arguments that led to (3.1); that is,

$$\overline{\rho e''u_{k,k}''} \simeq -\vartheta_k^T\bar{\rho}_{,k}/\bar{\rho}, \quad \overline{\rho'u_{k,k}''} \simeq \overline{u_k''}\bar{\rho}_{,k}. \tag{3.9}$$

For the density dilatation, the fluctuating conservation of mass equation was multiplied by ρ' and averaged. A comparison to the DNS data in figure 1(a) indicated that these models were qualitatively correct. An algebraic model was derived for (3.8) by recalling that $\bar{\rho}\overline{e''} = -\overline{\rho'e''}$, which allowed for the definition of a correlation coefficient. Performing the operations led to $(\bar{\rho}\overline{e''}) \approx -[\tau_{kl}^T\tilde{u}_{l,k} + (\bar{\rho}\tilde{e}_{,k} + \bar{p}\bar{\rho}_{,k}/\bar{\rho})\overline{u_k''}]\tau_{e''}$, where $\tilde{u}_{k,k}\overline{\rho'p'}$ and M were neglected. To close this term, the following truncation model for the mean Favre velocity fluctuation was derived from the conservation of momentum

$$D\bar{\rho}\overline{u_i''}/Dt = -\bar{\rho}\tilde{u}_{k,i}\overline{u_k''} + \overline{\rho u_i''u_{k,k}''} - \left(\tau_{ik}^T\bar{\rho}_{,k} - \overline{p'\rho_{,i}'} - \overline{\tau_{ki,k}'\rho'}\right)/\bar{\rho} + D_u, \tag{3.10}$$

where the triple and diffusion terms are grouped in D_u. The second and third terms cancel under the assumptions that led to (3.1). Following the arguments that led to (3.3), the fourth term was reduced to second-order diffusion. Since, all three terms in this expression are diffusion, the algebraic truncation is $(\tau_{u''}\tilde{u}_{k,i} + \delta_{ik})\overline{u_k''} \approx D_u$, where D_u denotes all of the second-order diffusion and third-order source terms. This result suggested that the mean Favre fluctuation was of the order of diffusion for flows that meet the assumptions leading to (3.1). Thus, neglecting this term in the mean energy fluctuation equation resulted in the following expression for b_i

$$b_i = \tau_{ik}^T\tilde{\psi}_{,k} + \tau_{kl}^T\tilde{u}_{l,k}\bar{p}_{,i}\tau_{e''}/\bar{\rho}, \tag{3.11}$$

where $\tau_{e''} \approx \sigma_{e''}k^T/\varepsilon$, and $\sigma_{e''}$ is a mechanical non-equilibrium modelling constant.

3.3. *Model constant σ_ϑ*

To set the constant σ_ϑ, the model was examined in the logarithmic region of a zero-pressure gradient turbulent boundary layer. For a boundary layer flow, where the principal strain rate is given by $\tilde{u}_{1,2}$, the model reduces to

$$\vartheta_1^T \simeq \tau_{12}^T\tilde{h}_{,2}\tau_\vartheta - \tau_{22}^T\tilde{h}_{,2}\tilde{u}_{1,2}\tau_\vartheta^2; \quad \vartheta_2^T \simeq \tau_{22}^T\tilde{h}_{,2}\tau_\vartheta. \tag{3.12}$$

Combining (3.2) with $q_i^T = \vartheta_i^T + \overline{p'u_i''} + \bar{p}\overline{u_i''}$ resulted in $q_i^T = \gamma\vartheta_i^T$, where $\gamma = \bar{C}_p/\bar{C}_v$ which is a function of temperature. Thus, in the near-wall region, the energy equation reduces to $\vartheta_2^T \approx q_{wall}/\gamma$. The time scale was estimated as $\tau_u = k^T/\epsilon \approx \mu_T/f_\mu C_\mu \rho k^T$,

where f_μ is a near-wall correction and C_μ is a constant ($= 0.09$). This relation results from the turbulence viscosity associated with $k - \epsilon$ models (Jones & Launder 1972). The Bradshaw, Ferrie & Atwell (1967) model was used to further simplify the time scale. The relation was multiplied by the van Driest damping factor d to extend the applicability to the wall, i.e.

$$\tau_{12}^T \approx a_1 d\bar{\rho}k^T. \tag{3.13}$$

In the above relation, $d = 1 - e^{-x_2^+/A^+}$, $x_2^+ = \rho_w u_\tau x_2/\mu_w$, $u_\tau = (\tau_w/\rho_w)^{1/2}$ and $A^+ = 26.0$. This relation is compared to DNS data in figure 1(b). With this, $\tau_u \approx a_1 d/f_\mu C_\mu \tilde{u}_{1,2}$. The gradient $\tilde{\psi}_{,2}$ was evaluated in the logarithmic region as $\tilde{h}_{,2} = -h_\tau/\kappa_T x_2$. Also, in this region, $\tilde{u}_{1,2} = u_\tau/\kappa x_2$, and d and f_μ are both $\simeq 1$. Noting that $h_\tau/u_\tau = q_w/\tau_w$, then the energy flux relation was reduced to $\vartheta_2^T \approx -(\tau_{22}^T/\tau_w)(\kappa/\kappa_T)(a_1\sigma_\vartheta/C_\mu)q_{wall}$. The first factor was written as $-\tau_{22}^T/\tau_w = 1/\overline{u_2'^{+2}}$, which is approximately constant at 0.75–0.85 within the logarithmic region (Barrett & Hollingsworth 2003). Thus, equating this expression to q_{wall}/γ resulted in $\sigma_\vartheta \approx (C_\mu/\gamma a_1)(\kappa_T/\kappa)(1/\overline{u_2'^{+2}})$, where $\kappa_T/\kappa \approx 1.1$–$1.2$ for gases and $a_1 = 0.27$–0.30 for high-Reynolds-number boundary layers. With these values, $\gamma\sigma_\vartheta \approx 0.25$–$0.32$. Comparing with the Launder (1988) model, it is readily seen that C_T corresponds to $\gamma\sigma_\vartheta$. Hence, the present model is consistent with the low-speed class of algebraic models for zero-pressure gradient flows with constant specific heats.

3.4. *Discussion of the model*

The algebraic energy flux model described in §§ 3.1–3.3 was developed specifically for high-speed shear flows, where compressibility effects are explicit in the dilatation models as shown in figure 1(a). The remaining simplifications translated into neglecting inhomogeneous terms. For example, the state equation simplifications to the pressure scrambling term resulted in the omission of an explicit sink term. Hence, when the velocity is constant, a_{ik} reduces to $\tau_\vartheta^{-1}\delta_{ik}$, and the energy flux dynamics are controlled by the Reynolds stress model and the thermal gradients; this case was not examined in detail here.

To better understand the differences between the present and gradient diffusion models, the two were compared for boundary layer flows. The analysis was facilitated by writing the turbulence viscosity as $\mu_T = f_\mu C_\mu \tau_{12}^T \tau_u/a_1 d$; this relation stemmed from the arguments in the previous section. Equating the two models led to $Pr_T = -(\tau_{12}^T/\tau_{22}^T)(C_\mu/\gamma\sigma_\vartheta a_1)(f_\mu/d)$. This expression was simplified with the following empirical relation:

$$\tau_{12}^T/\tau_{22}^T \approx -C/d, \tag{3.14}$$

where C is a constant and d is the van Driest damping factor. The van Driest damping factor was included to incorporate the correct near-wall asymptotic behaviour, that is, $u_1'' \sim x_2$ and $u_2'' \sim x_2^2$ (Lai & So 1990). With this behaviour, $\tau_{12}^T/\tau_{22}^T \sim x_2^{-1}$ as $x_2 \to 0$. The van Driest damping factor introduces the correct asymptotic behaviour near the wall. The constant C is nominally 0.6–0.8 for a number of shear flows. A comparison of (3.14) to DNS data, given in figure 1(b), demonstrated that the model produced the correct behaviour across the boundary layer. For this comparison, C was set to 0.68. The second factor $(C_\mu/\gamma\sigma_\vartheta a_1)$ is a constant, which is near unity for diatomic gases. Hence, a modified turbulent Prandtl number was derived as

$$Pr_T \simeq Pr_T^\infty/d_T, \tag{3.15}$$

where $Pr_T^\infty \equiv CC_\mu/\gamma\sigma_\vartheta a_1$, which is a constant in the range of 0.6–1.0 for diatomic gases. The term in the denominator of (3.15) is given by quotient $d_T = d^2/f_\mu$. Since f_μ is an empirical function used to correct the eddy viscosity near the wall, it was believed that this formulation may result in non-physical behaviour. Hence, the following model was proposed: $d_T = 1 - e^{-x_2^+/B^+}$, where B^+ was selected at 12.0 to fit the data in figure 1(*c*). Also, based on the comparison, Pr_T^∞ was set to 0.75. The agreement between the model, labelled 'Present theory', and the data was considered qualitatively good. Physically, these arguments suggest that the near-wall behaviour of the gradient diffusion and algebraic truncation models differ. Specifically, q_2 in the gradient diffusion model goes as x_2^3 as $x_2 \to 0$, where q_2 goes as x_2^4 for the algebraic models. Applying a Taylor series to the enthalpy fluctuations in the near-wall region indicates that the near-wall scaling of q_2 goes as $f_1 x_2^3 + f_2 x_2^4$ (Abe & Suga 2000). Since the prefactor f_1 is proportional to the mean enthalpy gradient, the first term is zero for adiabatic wall flows. The adiabatic wall DNS data of Pirozzoli *et al.* (2004) confirmed the x_2^4 dependency. Apparently, based on the comparisons in § 5, the latter term scaling also prevails for flows with heat transfer. Modifying Pr_T via (3.15) produces this behaviour.

Lastly, the Reynolds analogy was estimated for the present algebraic model as $2S_t/C_f \simeq \kappa_T/\kappa$, where the Stanton number and skin friction coefficient are given by $q_w/\rho_e U_e(h_w - h_{aw})$ and $\tau_w/\frac{1}{2}\rho_e U_e^2$, respectively. The observed range of κ_T/κ is 1.1–1.2, which indicates that the present Reynolds analogy expression is consistent with a large volume of empirical data across a wide range of speeds (e.g. see Cary 1970).

3.5. *A Comment towards pressure gradient flows*

To appreciate the role of the pressure gradient terms, the model was simplified for the case of a two-dimensional variable pressure gradient boundary layer. The resulting transverse energy flux is given by $\vartheta_2^T \simeq (\tau_{22}^T \tilde{h}_{,2} - \tau_{12}^T \bar{p}_{,1}/\bar{\rho})\tau_\vartheta$. To arrive at this form, it was assumed that the principal strain rate $\tilde{u}_{1,2}$ was much larger than the extra strain rates and $\bar{p}_{,2} \approx 0$. The non-dimensional parameter $B \equiv \bar{\rho}^{-1}\bar{p}_{,1}/\tilde{h}_{,2}$ was defined to characterize the relative importance of the pressure gradient for this as well as the other components. For many shear layer problems, $B \ll 1$. For example, B varied from $\sim 10^{-5}$ to $\sim 10^{-3}$ for the largest pressure gradient studied by Huora & Nagano (2006), corresponding to a Clauser (1956) pressure gradient parameter of 4.0. Hence, the pressure gradient terms in (3.5) and (3.11) were assumed negligible for most problems. A possible exception includes the strong gradients associated with high-speed flow. Moreover, at hypersonic conditions, the thermal gradients are reduced as the boundary layer thickness is increased with the Mach number. For the hypersonic expansion study of Bloy (1975), B was crudely estimated at ~ 0.1. Thus, the pressure gradient limitations of the present model require further study and calibration of $\sigma_{e''}$ requires a specifically designed high-Mach-number experiment.

4. Simulation methods

4.1. *Physical models*

The present algebraic model, (3.6), (3.7) and (3.11) with $\gamma\sigma_\vartheta = 0.28$; the modified gradient diffusion model, (3.11) with $Pr_T^\infty = 0.75$, $B^+ = 12$; the standard gradient diffusion model, with $Pr_T = 0.9$; and the algebraic models of Abe & Suga (2000) ($C_T = 0.4$), Daly & Harlow (1970) ($C_T = 0.3$) and Launder (1988) were examined. Since the goal of the present study was the advancement of the heat flux model, the test cases were limited to zero-pressure gradient flows, where an established two layer model for the Reynolds shear stress ($\tau_{12}^T = \mu^T \tilde{u}_{,2}$) was available. In the inner region,

the turbulence viscosity was computed with the Prandtl (1904) mixing length model and the van Driest (1956) near-wall damping function, that is, $\mu_i^T = \bar{\rho}\kappa^2 x_2^2 d^2 \tilde{u}_{1,2}$. In the outer region, the Clauser (1956) model was used with the Klebanoff (1955) intermittency correction, that is, $\mu_o^T = C_C \bar{\rho} U_e \delta_k^* \cdot [1 + C_K(x_2/\delta)^{n_k}]^{-1}$, where δ_k^* is the kinematic displacement thickness. The model constants were set to established values in the literature. Specifically, $\kappa = 0.41$, $A^+ = 26.0$, $C_C = 0.018$, $C_\mu = 0.09$, $a_1 = 0.28$, $C = 0.68$, $n_K = 6.0$ and $C_K = 1.2$ (this constant was re-tuned to match Pirozzoli *et al.* 2004 and Horstman & Owen 1972). The transverse normal stress τ_{22}^T was computed from the Reynolds stress with the empirical model described in §3.4; the quotient d^2/f_μ was modelled as d_T.

For the test cases presented here, the medium was air or helium. The air model was based on a mole fraction composition of 78 % N_2, 21 % O_2 and 1.0 % Ar. The temperature dependency of the specific heats was computed following Vincenti and Kruger (1965). The viscosity was computed following Roy & Blottner (2006). The molecular thermal conductivity was computed as $k = C_p/Pr$, where the molecular Prandtl number Pr was set to 0.71. Helium was treated as a calorically perfect gas. The viscosity was computed following Miller & Maddolon (1970). The molecular Prandtl number was set to 0.69.

4.2. *Finite difference models*

The model assessment was performed using the two-dimensional boundary layer equations (Prandtl 1904). An upwind finite difference scheme was used for the axial x_1 derivatives, and central differences were used for the transverse x_2 derivatives. To produce a stable solution, a downwind difference was used for the transverse mass flux in the conservation of mass equation. Variable grid spacing was used. A space-marching predictor–corrector solution procedure was employed, where for the predictor step, the coefficients in the finite difference equations were evaluated using the solution from the previous plane. For the corrector step, the coefficients were evaluated with the results from the predictor step. The above algorithm was not fully implicit, where treating the turbulence a source reduced the stability of the program.

The solutions were initiated with a parallel flow laminar similarity solution at an axial location of 1.0 % of the plate length or the transition location if provided. This was found to increase stability. An extrapolation boundary condition was used for the upper boundary. For the lower boundary, a no-slip isothermal wall was enforced. The solutions were marched until the predicted momentum thickness matched that of the test case.

Grid convergence was ensured, where solutions were run on the following grids 7500×50, 15000×75 and $25\,000 \times 100$. The maximum difference between solutions on these grids was 0.25 %, which was deemed acceptable for the model comparison studies. Consistency was validated with exact laminar similarity solutions, where solutions agreed to within 0.3 %

5. Model evaluation results

The primary model development testbed was the DNS data of Pirozzoli *et al.* (2004) shown in figures 2(*a*) and 2(*b*). The mean velocity profiles (figure 2*a*) for all of the models were in excellent agreement with the data. The constant turbulent Prandtl model temperature, $\Theta = (T_w - \bar{T})/(T_w - T_\infty)$, results agreed well with the DNS data in the outer region. However, in the region between $x_2^+ = 10$ and 200, Θ was underpredicted, where the largest difference was about 15 %. The temperature profiles for the modified turbulent Prandtl and the four algebraic models were within 3 %
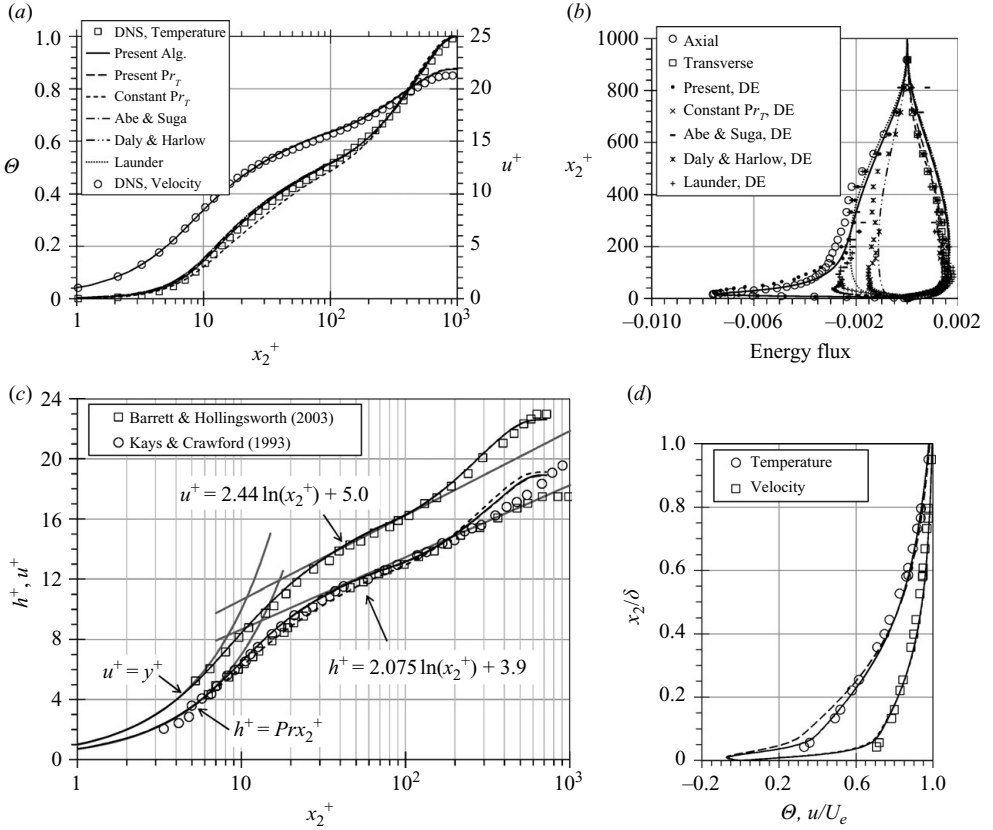
FIGURE 2. Model comparison. (*a*) DNS data of Pirozzoli *et al.* (2004), $M = 2.25$, Air, $T_w/T_{aw} = 1.0$, $Re = 4000$; (*b*) DNS axial and normal energy flux normalized by free stream conditions (legend continued from (*b*), DE indicates model evaluated with DNS data directly); (*c*) low-speed boundary layer with heat transfer (Barrett & Hollingsworth 2003 and Kays & Crawford 1993); (*d*) $M = 11.8$, He, $T_w/T_{aw} = 0.56$, $Re = 18\,000$ (Watson 1978).

of the DNS data across the entire boundary layer. Similar trends were observed when evaluating the models for the Mach 2.8 adiabatic wall experiments described in Bowersox (1996).

The comparisons of the modelled energy flux to the DNS data are given in figure 2(*b*). In addition to the numerical simulations, the model formulations were directly evaluated with the DNS data; these data are also included in figure 2(*b*). Focusing on the DNS evaluations (labelled DE), the Abe & Suga (2000) and Launder (1988) axial flux results agreed well with the data for x_2^+ greater than about 100. Below this region, the models did not capture the observed peak. Abe & Suga (2000) showed slightly better results in this region as the model was adjusted to depend on the axial shear stress. The Daly & Harlow (1970) model underpredicted the axial flux across the boundary layer. Following the arguments in § 3.4, the near-wall scaling for q_1 goes as x_2^3 for adiabatic wall flows. To achieve this scaling, the modelled axial component for the present model was divided by $1 - e^{x_2^+/B_1^+}$, where B_1^+ was selected at 95 to capture the near-wall peak shown in figure 2(*b*). This factor asymptoted to unity near $x_2^+ = 250$. With this correction, the present model agreed well with the data across the entire boundary layer. The corresponding numerical simulation axial flux results shown in figure 2(*b*) followed the trends established by the DNS model

evaluations. The differences between the models for the transverse component were subtle, and the corresponding differences in the temperature profiles were the result of the near-wall behaviour described in §3.4. Similar agreement was seen for the experiments in Bowersox (1996).

The present and gradient diffusion models were also compared to the low-speed data of Barrett & Hollingsworth (2003) and Kays & Crawford (1993) in figure 2(*c*). The velocity profiles for the three models were in excellent agreement with the data. The present model temperature results were approximately 10 % higher than the constant turbulent Prandtl model in the $x_2^+ = 10$ and 200 region. However, the experimental data spanned the model differences.

Lastly, the models were compared to the hypersonic data of Watson (1978) in figure 2(*d*). The constant turbulent Prandtl number model temperature predictions were up to 20 % off in the $x_2/\delta = 0.05$ to 0.35 region of the boundary layer. The temperature profiles with the present models were in much better agreement across the entire boundary layer. Similar findings were observed for the Mach 7.1, $T_w/T_{aw} = 0.52$ air study of Horstman & Owen (1972).

6. Conclusions

An algebraic truncation model was derived for high-speed shear layers. The model appeared to provide significant improvements in the temperature predictions over the constant turbulent Prandtl number model, when compared to experimental and DNS data over a Mach number ranging from 0.02 to 11.8. The improvements, up to 20 %, occurred in the $x_2^+ = 10$ to 200 region of the boundary layer, and were most pronounced in the supersonic and hypersonic boundary layers. Analyses of the algebraic model resulted in a Reynolds analogy factor that was proportional to the ratios of the slopes of the temperature and velocity profiles in the logarithmic region of the boundary layer, which is consistent with numerous studies within the literature.

The inclusion of compressibility led to explicit pressure gradient dependency with the algebraic model. Analyses indicated that if $B \equiv \bar{\rho}^{-1}\bar{p}_{,1}/\tilde{h}_{,2}$ is small then the pressure gradient terms are negligible. For most flows, this parameter is very small, however for high-speed flow, this term may become significant. Additional experiments are required to better understand the pressure gradient limitations of the present models.

The algebraic model produced accurate predictions of the heat flux vector as compared to DNS results. An important inference from the analysis was that the near-wall behaviour of the algebraic model for q_2 agreed with expected scaling, where the gradient diffusion model did not. This comparison led to a slight modification of the turbulent Prandtl number. Specifically, $Pr_T \simeq Pr_T^\infty/d_T$, where Pr_T^∞ is a constant near 0.75 and d_T is similar the van Driest damping function. The resulting model produced results that were in agreement with the algebraic model for the transverse component of the heat flux.

REFERENCES

ABE, K. & SUGA, K. 2000 Towards the development of a Reynolds-averaged algebraic turbulent scalar-flux model. *Intl J. Heat Fluid Flow* **22**, 19–29.

BARRETT, M. & HOLLINGSWORTH, K. 2003 Heat transfer in turbulent boundary layers subjected to free-stream turbulence Part 1. Experimental results. *J. Turbomach.* **125**, 232–241.

BLOY, A. 1975 The expansion of a hypersonic turbulent boundary layer at a sharp corner. *J. Fluid Mech.* **67**, 647–655.

BOWERSOX, R. 1996 Combined laser doppler velocimetry and cross-wire anemometry analysis for supersonic turbulent flow. *AIAA J.* **31**, 2269–2275.

BRADSHAW, P., FERRIE, D. & ATWELL, N. 1967 Calculation of boundary layer development using the turbulent energy equation. *J. Fluid Mech.* **28**, 593–616.

CARY, A. 1970 Summary of available information on Reynolds analogy for zero-pressure-gradient, compressible turbulent-boundary-layer flow. *Tech. Rep.* TN D-5560. NASA.

CLAUSER, F. H. 1956 The turbulent boundary layer. In *Advances in Applied Mechanics* (ed. H. L. Drydek & Th. von Karmax), vol. 4, chap. 1, pp. 1–51. Academic Press.

DALY, B. & HARLOW, F. 1970 Transport equations in turbulence. *Phys. Fluids* **13**, 2634–2649.

VAN DRIEST, E. 1956 On turbulent flow near a wall. *J. Aeronaut. Sci.* **23**, 1007–1012.

FAVRE, A. 1969 Statistical equation of turbulent gases. In *Problems of Hydrodynamics and Continuum Mechanics*, pp. 231–266. SIAM.

GIRIMAJI, S. & BALACHANDER, S. 1998 Analysis and modelling of bouyancy-generated turbulence using numerical data. *Intl J. Heat Mass Transfer* **41** (6–7), 915–929.

HORSTMAN, C. & OWEN, F. 1972 Turbulent properties of a compressible boundary layer. *AIAA J.* **10** (11), 1418–1424.

HUORA, T. & NAGANO, Y. 2006 Effects of adverse pressure gradient on heat transfer in thermal boundary layer. *Intl J. Heat Mass Transfer* **27**, 967–976.

JONES, W. & LAUNDER, B. 1972 The prediction of laminarization with a two-equation model of turbulence. *Intl J. Heat Mass Transfer* **15**, 301–314.

KAYS, W. & CRAWFORD, M. 1993 *Convective Heat and Mass Transfer*. McGraw-Hill.

KLEBANOFF, P. 1955 Characteristics of turbulence in a boundary layer with zero pressure gradient. *Tech. Rep.* 1247. NACA.

LAI, Y. & SO, R. 1990 Near-wall modelling of turbulent heat fluxes. *Intl J. Heat Mass Transfer* **33** (7), 1429–1440.

LAUNDER, B. 1976 Heat and mass transfer. In *Topics in Applied Physics, Turbulence* (ed. P. Bradshaw), chap. 6, pp. 232–287. Springer-Verlag.

LAUNDER, B. 1988 Computation of convective heat transfer in complex flows. *ASME* **110**, 1112–1128.

MILLER, C. & MADDOLON, D. 1970 Errors in free stream Reynolds number of helium wind tunnels. *AIAA J.* **8**, 968–970.

MORKOVIN, M. 1961 Effects of compressibility on turbulent flows. In *Mécanique de la Turbulence* (ed. A. Favre), pp. 367–379. Centre National de la Recherche Scientifique, Paris.

PIROZZOLI, S., GRASSO, F. & GATSKI, T. 2004 Direct numerical simulation and analysis of a spatially evolving supersonic turbulent boundary layer at M = 2.25. *Phys. Fluids* **13** (3), 530–545.

POPE, S. 1983 Consistent modelling of scalars in turbulent flows. *Phys. Fluids* **26**, 404–408.

PRANDTL, L. 1904 Über flüssigkeitbewegung bei sehr kleiner reibung. In *Proc. 3rd Intl Math. Congr*. Heidelberg, Germany.

RISTORCELLI, J. 1993 A presentation for the turbulent mass flux contribution to the Reynolds-stress and two-equation closures for compressible turbulence. *Tech. Rep.* CR 191569. NASA LARC, Hampton, VA.

ROY, C. & BLOTTNER, F. 2006 Review and assessment of turbulence models for hypersonic flows. *Prog. Aerosp. Sci.* **42**, 469–530.

SNIJDERS, A., KOPPIUS, A. & NIEUWVELT, C. 1983 An experimental determination of the turbulent Prandtl number in the inner boundary layer for air over a flat plate. *Intl J. Heat Mass Transfer* **26**, 425–431.

VINCENTI, W. & KRUGER, C. 1965 *Introduction to Physical Gas Dynamics*, chap. 4, pp. 86–151. Krieger Publishing Co.

WATSON, R. 1978 Characteristics of Mach 10 transitional and turbulent boundary layers. *Tech. Rep.* TP 1243. NASA LARC, Hampton, VA.

WIKSTROM, P., WALLIN, S. & JOHANSSON, A. 2000 Derivation and investigation of a new explicit algebraic model for the passive scalar flux. *Phys. Fluids* **12**, 688–702.